

Does vibration superimposed on low-level isometric contraction alter motor unit recruitment strategy?

Lin Xu¹, Francesco Negro², Yu Xu¹, Chiara Rabotti¹, Goof Schep³, Dario Farina⁴, and Massimo Mischì¹

¹Faculty of Electrical Engineering, University of Technology Eindhoven, Eindhoven, The Netherlands

²Department of Clinical and Experimental Sciences, Università degli Studi di Brescia, Brescia, Italy

³Máxima Medical Center, Veldhoven, The Netherlands

⁴Department of Bioengineering, Imperial College London, London, England

E-mail: l.xu@tue.nl

Abstract. Objective. Beneficial effects, including improved muscle strength and power performance, have been observed during vibration exercise (VE) and partially ascribed to a specific reflex mechanism referred to as Tonic Vibration Reflex (TVR). TVR involves motor unit (MU) activation synchronized and un-synchronized with the vibration cycle; this suggests VE to alter the temporal MU recruitment strategy. However, the effects of VE on MU recruitment remain poorly understood. This study aims to elucidate the influence of VE on MU recruitment indirectly, by investigating the effects of low-intensity VE on muscle activation. Approach. Twenty volunteers performed isometric contractions on the biceps brachii of the right arm at a baseline (low) force equal to 30% of the maximum voluntary contraction without vibration (control) and with vibration at 20, 30, 40, and 55 Hz. Three vibration amplitudes were employed at 12.5%, 25%, and 50% of the baseline. Mean muscle-fiber conduction velocity (mCV), mean frequency (MF), and root mean square (RMS) value were estimated from surface electromyography as indicators of the alteration in MU recruitment strategies. Main results. The mCV estimates during VE were significantly ($p < 0.05$) higher compared to the control condition. Furthermore, six VE conditions produced significantly larger RMS values compared to control condition. The estimated MF did not show any consistent trend. Significance. These results suggest that vibration superimposed on low-level isometric contraction alters the MU recruitment strategy, activating larger and faster MUs.

Keywords: Vibration Exercise, Electromyography, Motor Unit, Recruitment pattern, Tonic Vibration Reflex.

1. Introduction

Vibration exercise (VE) has become a popular training methodology in rehabilitation programs, athlete training, and leisure sports. It has been suggested that VE has beneficial effects by improving muscle strength, body balance, and bone density (Bosco et al. 1998, Abercromby et al. 2007). Whole body vibration platforms are widely used vibration training devices which are designed for the lower limbs (Cardinale & Lim 2003). Other vibration exercise systems, such as vibrating dumbbells, vibrating barbells, and force-modulated vibrating systems, have also been proposed to train the upper limbs (Poston et al. 2007, Bosco et al. 1999, Mischi & Cardinale 2009, Xu, Cardinale, Rabotti, Beju & Mischi 2016).

The beneficial effects of VE have been related to a specific reflex mechanism referred to as Tonic Vibration Reflex (TVR) (Eklund & Hagbarth 1966, Hagbarth & Eklund 1966, Bongiovanni et al. 1990). TVR is known to be evoked by mechanical vibration applied directly to the muscle belly or tendon, which activates the Ia fibers (Martin & Park 1997). Apart from the modulation of Ia-afferents, TVR may also be adjusted by variations in the spindle sensitivity through γ control (Matthews 1966, Ribot-Ciscar et al. 2000). Recent studies suggested that indirect application of vibration to the muscle by force modulation may also elicit TVR (Xu et al. 2015).

TVR determines alteration in the motor unit (MU) recruitment pattern resulting from vibration. Muscle force is determined by MU recruitment and rate coding, i.e., modulation of the MU discharge rate (Sörnmo & Laguna 2005). When force increases, MUs are recruited following the Henneman's Size Principle (E Henneman & Carpenter 1965) and at the same time, the firing rate of the earlier recruited MUs increases. When nearly all MUs are recruited, rate coding becomes the prominent mechanism to increase force.

TVR is a reflex that determines MU synchronized activation, asynchronized with the vibration cycle (Hori et al. 1989, Romaguère et al. 1991); MU synchronization refers to simultaneous discharge of action potentials by different motor neurons (Semmler 2002). The effects of vibration on MU recruitment are poorly understood. Furthermore, recent work suggested that the central nervous system may modulate VE (Krause et al. 2016), which can also influence the MU recruitment strategies.

Surface electromyography (sEMG) is a non-invasive method to record the action potentials of contracting muscle fibers. The measured sEMG signal results from a spatial and temporal superimposition of the action potentials of the active MUs within the detection volume. However, by signal processing techniques, indirect information reflecting MU recruitment strategies can still be extracted from the global sEMG. Specifically, the mean conduction velocity (mCV) of the active muscle fibers can be reliably measured from multi-channel EMG (Farina, Zagari, Gazzoni & Merletti. 2004) and is associated to MU recruitment (Del Vecchio et al. 2017). mCV depends on the diameter of muscle fibers, pH, and ion concentration (Brody et al. 1991, Morimoto

& Masuda 1984). For example, Arendt-Nielsen *et al.* observed an increase in mCV when the level of voluntary contraction increased (Andreassen & Arendt-nielsen 1985), an indication of progressive recruitment of MU with faster muscle fibers (Del Vecchio *et al.* 2017). Other variables extracted from the surface EMG, such as mean power spectral frequency (MF) and root mean square (RMS) value are also frequently used for inferring MU properties, although with severe limitations (Farina, Merletti & Enoka 2004).

Previous studies reported increased sEMG RMS during VE (Bosco *et al.* 1999, Roelants *et al.* 2006), and others have shown estimates of global sEMG features during vibration (Xu, Rabotti & Mischi 2016, Sammali *et al.* 2018). However, there are no previous studies that assessed MU recruitment by mCV analysis during vibration. Therefore, the effect of vibration on MU recruitment is not fully understood. This study aims at investigating the influence of vibration on the strategies of MU recruitment by the analysis of multi-channel EMG. For this purpose, since recruitment is dominant during low-level contractions (E Henneman & Carpenter 1965), we adopted a baseline force level of 30% of the Maximum Voluntary Contraction (MVC) force. A force-modulated VE system previously developed (Xu *et al.* 2013) was used to induce vibration on the baseline contraction.

2. Method

2.1. Subjects

Twenty healthy right-handed subjects participated in this study. The participants reported no neuromuscular disorder, no history of upper extremity surgery nor injury. The experimental protocol was explained clearly to the subjects and written informed consent was obtained from every subject prior to participation in the study. The test procedures were approved by the ethical committee in Máxima Medical Center (MMC, Veldhoven, the Netherlands).

2.2. Experimental setup

2.2.1. Vibration system Figure 1 (a) illustrates the scheme of the adopted VE system which was previously presented in Xu (Xu *et al.* 2013). The core component of this system is a motor (MSK060C, Bosch Rexroth, Boxtel, The Netherlands), which is able to generate a force combining a constant baseline and a superimposed sinusoidal vibration. An example of the output force is shown in Fig. 1 (b). The motor driver (IndraDrive HCS02, Bosch Rexroth, Boxtel, The Netherlands) is controlled through an analog function generator (PCI-5402, National Instruments, Austin, TX, USA) connected to a PC, where dedicated software is implemented in LabView[®] (National Instruments, Austin, TX, USA).

An aluminum bar is mounted perpendicular to the output shaft of the motor in order to apply a vertical force to the subject's arm. Then a cable and a handle connected

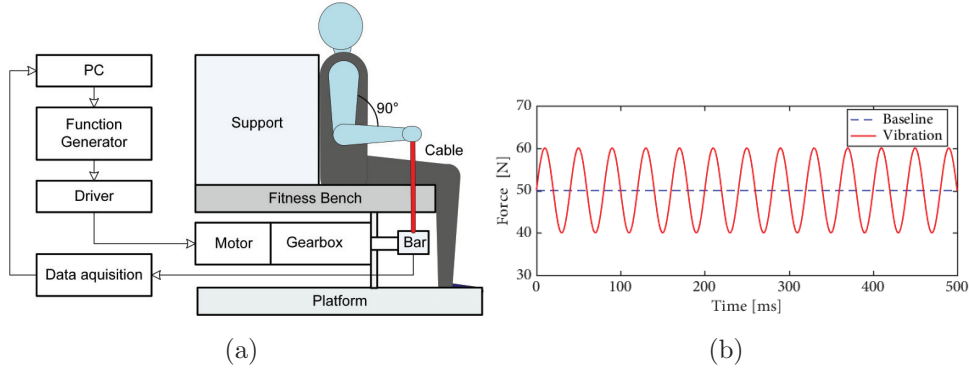


Figure 1. Scheme of the vibration system together with an example of its output force: a baseline superimposed with a 10-N sinusoidal vibration at 20 Hz.

to the bar are able to transfer the generated force to the subject. A LCAE-35kg load cell (Omega Engineering Inc, Stamford, Connecticut, USA) is embedded in the bar, which uses resistance-based force sensors in full bridge configuration to measure the force generated by the motor. The position of the bar, which represents the wrist position of the subject during VE, is measured by a rotary encoder embedded in the motor, providing visual feedback of the wrist position to the subject.

2.2.2. sEMG recording sEMG was recorded from the biceps brachii muscle of the subject's right arm using two electrode grids with their columns aligned with the muscle fiber direction (Fig. 2). The high-density electrode grid consisting of 8×8 Ag/AgCl electrodes is shown in Fig. 3. The inter-electrode distance and diameter of the grid was 8 mm and 4 mm, respectively. A circular (1-cm diameter) Ag/AgCl electrode was placed on the subject's right clavicle as ground. The measured signals were amplified and digitized using a 136 channel Refa amplifier (TMS International, Enschede, The Netherlands) and then transferred to the PC. The sampling frequency was 2048 Hz.

2.3. Measurement protocol

Prior to the measurements, the subject was first asked to perform 15 repetitions of biceps curl exercise using a 3 kg dumbbell for warming up. The next step was to measure the MVC of the subject using the load-cell embedded in the bar. The subject was instructed to sit on the fitness bench with his/her back straight and against the support while keeping the elbow angle at 90 degrees (Fig. 1). A visual feedback of the elbow angle, measured by the rotary encoder embedded in the motor, was provided on a screen to help the subject to maintain this position. During the measurement, the subject pulled the cable upwards with his/her maximum effort for three seconds while the bar of the experimental system was blocked. The force data were sensed by the load cell and recorded in LabView[®]. The MVC was measured three times with recovery time of 3 minutes. The maximum value of the three measurements was considered to be the reference MVC. The next phase consisted of the VE trials along with the sEMG



Figure 2. Position of the electrode grids during sEMG recording.

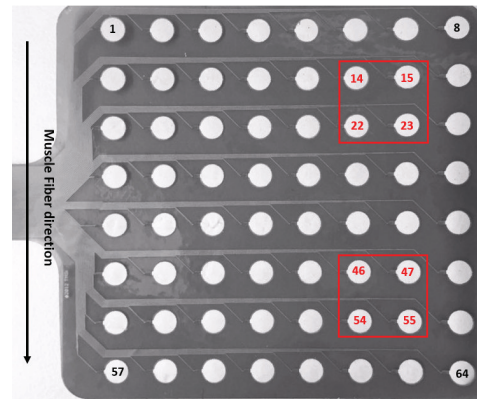


Figure 3. The high-density electrode grid and the two 4-channel sub-sets used to extract one bipolar signal for RMS and MF estimation.

recording. The subject maintained the same position as for the MVC measurement and performed 30-s isometric contractions. The baseline force was 30% of the MVC while the amplitude of the superimposed vibration was 12.5%, 25%, and 50% of the baseline. Those contractions were performed with no vibration (control condition), and vibration at 20, 30, 40, and 55Hz. As a result, 13 trials were performed in a random order. Between each trial, 2-minute recovery was taken.

2.4. Signal processing

2.4.1. Data preprocessing The acquired signals were processed in Matlab[®] (Matlab 2016b, The Mathworks, Natick, MA, USA). For each trial, the global features mCV, MF, and RMS were calculated as indicators of MU recruitment strategy. To avoid transient effects and the influence of fatigue, the data were extracted as the first ten seconds after a stable period of 2 s. After extraction of the desired segment of data, a quality check of the data was performed. Channel recordings with constant values (not recorded successfully) or more than 100 consecutive zeros were excluded. Subjects with more than 10 excluded channels in any trial were totally excluded from the analysis.

In general, a frequency band between 20 and 450 Hz is considered for sEMG analysis in the literature (Xu et al. 2015). However, in our study, several VE trials were performed at 20 Hz. Thus a frequency band from 15 to 450 Hz was considered in order to include 20 Hz while investigating the vibration effects. Since all the EMG features, mCV, MF, and RMS, can be calculated in the frequency domain, the frequency components between 15 to 450 Hz were directly extracted in the frequency domain. In order to remove the power-line interference, a bandwidth of ± 0.8 Hz around 50 Hz plus all the harmonics were excluded from the calculation by setting their amplitude spectrum to zero.

Furthermore, the sEMG spectrum estimated during VE shows sharp peaks at the vibration frequency (SP_{VF}) and, in some cases, its harmonics. Some studies interpreted

these SP_{VF} as motion artifacts (Fratini et al. 2009, Romano et al. 2018, Lienhard et al. 2015). However, other studies have associated those SP_{VF} to vibration-induced muscle activity and suggested to include them in the sEMG analysis (Xu et al. 2015, Ritzmann et al. 2010). In order to avoid any bias caused by these SP_{VF} on our results, the three sEMG global features were calculated both with and without including the frequency band (± 0.8 Hz) around the vibration frequency and its harmonics.

A bipolar signal was extracted for RMS, and MF estimation by taking the difference between the average of two sub-sets of 4 channels, channel 14, 15, 22, 23 and channel 46, 47, 54, 55, as shown in Fig. 3. For mCV estimation, the innervation zone of the muscle was first identified by visually checking the propagation direction of the sEMG signal. The channels located between the innervation zone and the tendon were then chosen to derive bipolar signals. The selected monopolar channels were normalized to obtain zero mean and unit variance. The bipolar signals were then obtained by subtracting the signals of adjacent rows in the same column. The derived bipolar signals were then used for mCV estimation. Figure 4 shows an example of the bipolar signals in one column.

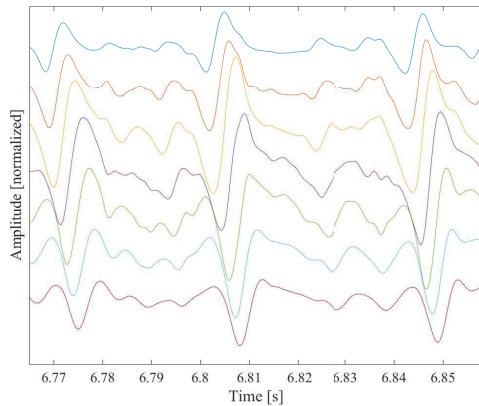


Figure 4. Example of bipolar sEMG signals measured along one column of the electrode grid without 50-Hz interference.

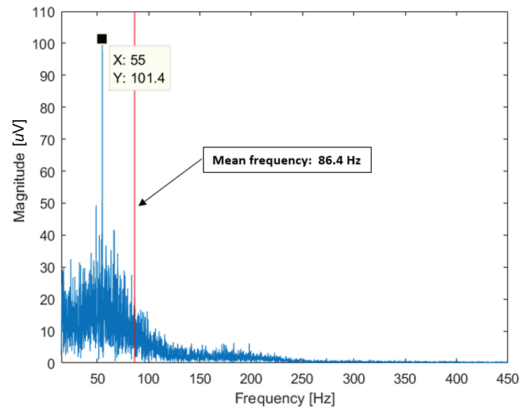


Figure 5. Example of sEMG amplitude spectrum estimated during VE at 55 Hz without 50-Hz interference.

2.4.2. mCV estimation Various approaches for estimating average muscle-fiber CV from sEMG have been proposed in literature, including estimation of spectral dips (Lynn 1979, Farina & Negro 2007a), phase difference (McGill & Dorfman 1984, Hunter et al. 1987), cross-correlation (Parker & Scott 1973), and maximum likelihood (ML) (Farina et al. 2001, Farina, Pozzo, Merlo, Bottin & Merletti 2004, Rabotti et al. 2010). A recent study also suggested a phase-lock-loop method for real-time mCV estimation (Xu et al. 2017). Among these methods, the ML method based on multichannel sEMG is the most popular one, enabling estimation of mCV with enhanced reliability (Farina & Merletti 2004).

In this study, the mCV was estimated using the multichannel ML method described in (Xu, Rabotti & Mischi 2016). In general, mCV is estimated by computing the ratio

between the inter-electrode distance and the delay between the sEMG waveforms (Farina et al. 2001, Naeije & Zorn 1983), which is given as:

$$\text{CV} = \frac{d \cdot f_s}{\theta}, \quad (1)$$

where d is the inter-electrode distance, f_s the sampling frequency, and θ the delay in samples. Since the inter-electrode distance and the sampling frequency are known a priori, the mCV estimation requires the estimation of θ only.

As the columns of the grid are aligned with the muscle fiber direction (Fig. 6), the signals recorded by the electrodes in the same column of the grid can be assumed to have the same shape while delayed by θ samples between adjacent rows. Taking a white, Gaussian noise w_{kl} with variance σ_{kl}^2 into consideration, the signal from the k^{th} row and l^{th} column, x_{kl} , can be modeled as

$$x_{kl}(n) = s_l[n - (i - 1)\theta] + w_{kl}(n), \quad n = 1, \dots, N; k = 1, \dots, R; l = 1, \dots, C \quad (2)$$

where k and l are the row and column indices, respectively, N the number of samples, R the number of rows, C the number of columns, and s_l the noise-free signal at column l .

The ML estimator of θ is derived by maximizing the posterior probability $p(\theta | \underline{x}_{11}, \dots, \underline{x}_{RC}, \underline{s}_l)$, where \underline{x}_{kl} and \underline{s}_l are the vector representations of $x_{kl}(n)$ and $s_l(n)$, respectively. Assuming a uniform prior probability $p(\theta)$, maximization of $p(\theta | \underline{x}_{11}, \dots, \underline{x}_{RC}, \underline{s}_l)$ corresponds to the maximization of the likelihood $p(\underline{x}_{11}, \dots, \underline{x}_{RC} | \theta, \underline{s}_l)$. The ML estimation of θ is then given by (Xu, Rabotti & Mischi 2016)

$$\hat{\theta} = \arg \max_{\theta} \left(\sum_{l=1}^C \sum_{k=1}^R \sum_{m=1}^R \frac{1}{2\pi} \int_{-\pi}^{\pi} X_{kl}(e^{j\omega}) X_{ml}^*(e^{j\omega}) e^{j(k-m)\theta\omega} d\omega \right), \quad (3)$$

where $*$ indicates the complex conjugate and $X_{kl}(e^{j\omega})$ and $X_{ml}(e^{j\omega})$ denote the Short-Time Fourier Transform (STFT) of $x_{kl}(n)$ and $x_{ml}(n)$, respectively. In (3), θ is calculated in the frequency domain; therefore, it is no longer constrained to integer values as in the time domain, increasing the time resolution of θ estimation.

The estimation of θ is performed by a two-level grid search as described in (Xu, Rabotti & Mischi 2016), which produces sufficient resolution for θ estimation while limiting the computational demand. In a first round, $\hat{\theta}_1$ is estimated by evaluating the integral in (3) in a limited range of θ with relatively large step size s_1 . A second round is used for a finer search with θ ranging from $\hat{\theta}_1 - s_1$ to $\hat{\theta}_1 + s_1$ with very small step size equal to 0.02 sample, leading to a resolution of 0.01 ms for the final θ estimation. The search interval for the first round can be determined by equation (1). Given the inter-electrode distance, 8 mm, and the sampling frequency, 2048 Hz, a θ ranging from 1 to 10 samples can produce mCV values from 1.64 to 16.4 m/s, which is sufficient to cover the CV range reported in the literature for the biceps brachii, i.e., 2-8 m/s (Davies & Parker 1987). The optimal step size for the first round, s_1 , is then obtained by minimizing the total number of search steps N_s in the two rounds, given by $N_s = (10 - 1)/s_1 + 1 + 2 \times s_1/0.02$. Setting the first derivative of N_s to zero, we obtain $s_1 = 0.3$ sample, resulting in 61 searching steps in total.

2.4.3. MF and RMS estimation The MF is estimated as the first statistical moment of the STFT amplitude spectrum. The RMS value of the sEMG is estimated in the frequency domain between 15 and 450 Hz using Parseval's equality.

2.5. Statistical Analysis

The features mCV, MF, and RMS were used in the statistical analysis. Two subjects were excluded from the analysis based on the exclusion criteria described in 2.4.1. One-sample Kolmogorov-Smirnov test suggested our data to be normally distributed. Our data were obtained by repeated measures from the same subject at different vibration amplitudes and frequencies. For each vibration amplitude, a one-way repeated-measures ANOVA was employed to assess the effect of the vibration frequency on the EMG features, with each EMG feature being the dependent variable and the vibration frequency the independent variable. Following the ANOVA, two post-hoc tests with different methods were performed for different objectives. The first post-hoc test aimed at assessing the difference between different vibration frequencies by using the Tuckey's method. However, the main objective of the present study was to investigate the effects of vibration on MU recruitment strategies; therefore, another post-hoc test using the Fishiers least significant difference (LSD) approach was adopted to test the difference between each vibration condition and non-vibration (control condition). Furthermore, the difference between vibration (average of all vibration conditions) and non-vibration (control condition) was also assessed by paired sample Student's t-test. For all the analysis, α was set to 0.05.

3. Results

3.1. mCV estimation

For the calculation including the SP_{VF} , the estimated mCV ranged from 3.0 to 6.5 m/s, in agreement with previous work (Davies & Parker 1987). Figure 6 (a) shows the mCV estimates. These results are separated in three groups with each group representing one vibration amplitude. For each vibration amplitude, the 5 bars represent the mCV estimates at different vibration frequencies: 0 (control condition), 20, 30, 40, and 55 Hz. All the vibration conditions produced increased mCV as compared to the control condition. The one-way repeated-measures ANOVA showed that at least one group was significantly different from all the others for vibration amplitudes at 25% and 50% baseline ($p < 0.01$). Conversely, no group is significantly different from all the other groups with vibration amplitude at 12.5% baseline ($p = 0.24$). The Tuckey's post-hoc test revealed that differences between different vibration frequencies (pairs) were not significant. However, the Fishiers LSD test revealed that mCV significantly increased during vibration with respect to baseline, except for the vibration at 20 Hz, 12.5% baseline. For all vibration amplitudes, the difference between vibration (average of four frequencies) and no-vibration (control condition) was significant ($p < 0.01$). Similar

results were observed for the mCV estimates when excluding the SP_{VF} (Fig. 6 b)).

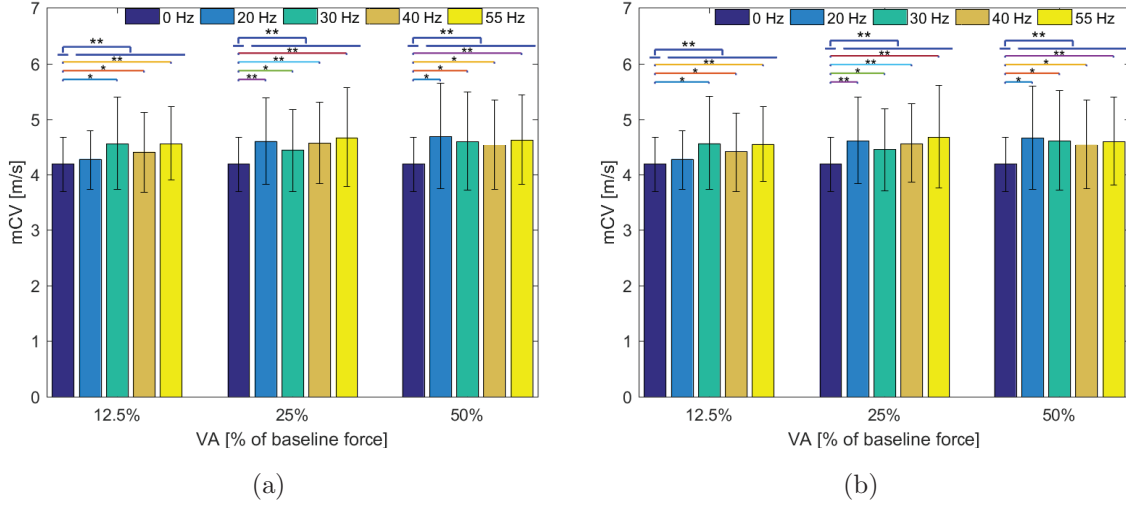


Figure 6. mCV estimation results: a) including vibration frequency; b) excluding vibration frequency. VA: vibration amplitude. * indicates significant level $p < 0.05$ obtained by the Fishier's LSD test; ** indicates significant level $p < 0.01$ obtained by the Fishier's LSD test.

3.2. MF estimation

Figure 5 shows an example of EMG amplitude spectrum together with the estimated MF for one VE trial at 55 Hz with amplitude 25% of the baseline. A sharp peak can be observed at the vibration frequency. The estimated MF is illustrated in the figure as a red vertical line located at 86.4 Hz.

The MF estimates from all the trials ranged from 73 to 115 Hz, in agreement with previous work (Li & Sakamoto 1996). The average MF results over all subjects are shown in Fig. 7. The MF estimates calculated with and without the SP_{VF} showed similar trends. As compared with the control condition, three VE conditions revealed an increase in the estimated MF while the remaining nine conditions showed a decrease in MF. These observed changes were however not significant.

3.3. RMS estimation

For the control condition, the estimated RMS value was $485 \pm 207 \mu V$. For the vibration conditions, the RMS values estimated including the SP_{VF} were similar as those estimated excluding the SP_{VF} . The RMS estimates during vibration were greater than at baseline, with the exception of vibration at 20 Hz, 12.5% of the baseline. The one-way repeated-measures ANOVA showed that, for each vibration amplitude, no group was significantly different from all the others. The Tuckey's test revealed no significant difference between different vibration frequencies. However, the Fishiers LSD test indicated 6 significantly different vibration conditions with respect to no vibration,

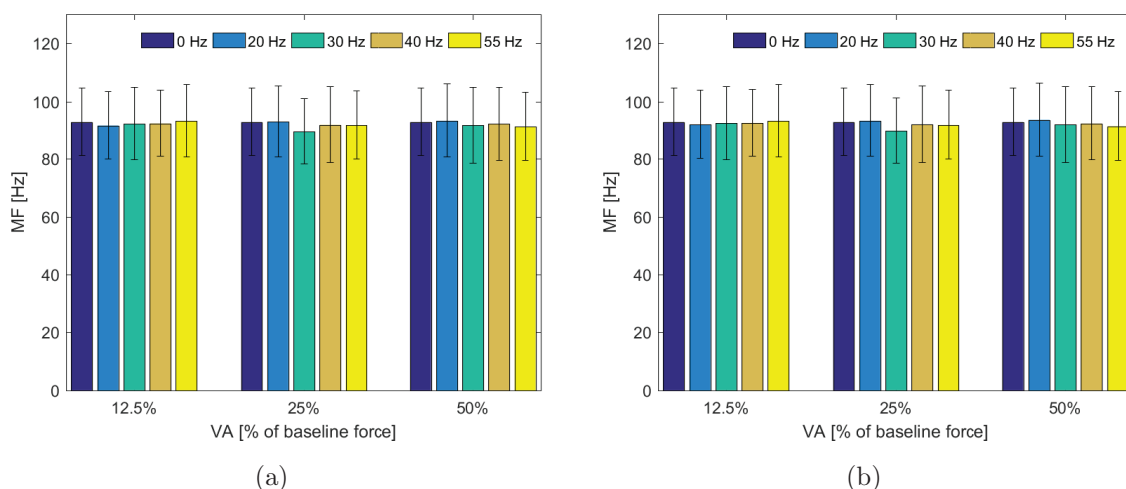


Figure 7. MF estimation results: a) including vibration frequency; b) excluding vibration frequency. VA: vibration amplitude.

as shown in Fig. 8. The differences between vibration (average of four frequencies) and no-vibration (control condition) were significant ($p < 0.01$) for vibration amplitude of 25% and 50% baseline. The p values between each vibration condition and control condition obtained by the Fishiers LSD test are shown in Fig. 9.

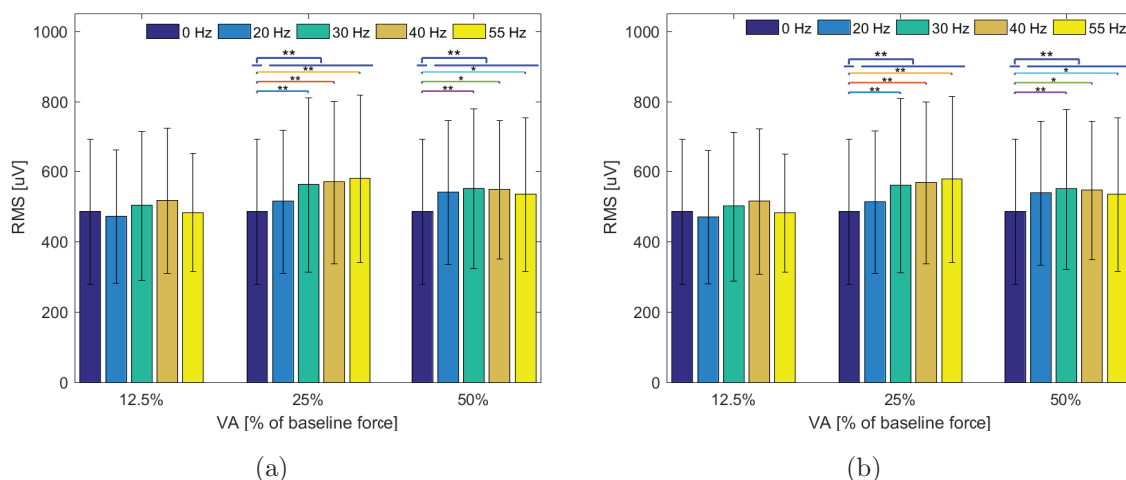


Figure 8. RMS estimation results: a) including vibration frequency; b) excluding vibration frequency. VA: vibration amplitude. * indicates significant level $p < 0.05$ obtained by the Fishier’s LSD test; ** indicates significant level $p < 0.01$ obtained by the Fishier’s LSD test.

4. Discussion

The influence of vibration on MU recruitment strategy during low-level isometric contraction was investigated by analyzing mCV, MF, and RMS of multichannel sEMG signals recorded from the biceps brachii muscle. The objective was to investigate the

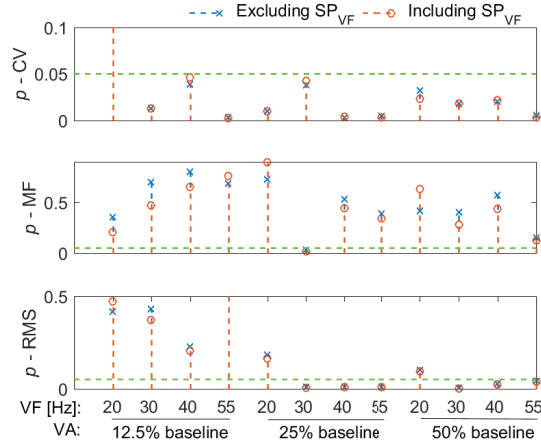


Figure 9. p values between each vibration condition and control condition obtained by the Fishiers LSD test. VF: vibration frequency; VA: vibration amplitude.

influence of VE on MU recruitment; therefore, we mainly focused on the difference between each vibration condition and the control condition.

The sEMG spectrum estimated during VE showed peaks at the vibration frequency and its harmonics, whose interpretation in terms of motion artifacts or muscle activity is still controversial. In order to avoid any bias caused by these SP_{VF} on our results, the EMG features were calculated with and without including these SP_{VF} . The estimated results were similar in all cases, indicating negligible influence of the SP_{VF} on the estimation of EMG features.

In the present study, bipolar derivations were used to calculate the EMG features. Since the bipolar signal was derived along the muscle fiber direction, it represents mainly a measure of amplitude difference in each MU action potential at two time points. The use of bipolar signals can remove most of the common mode potential and the cross talk from different muscles, therefore improving the signal-to-noise ratio. It is reported that bipolar EMG signals with normalization produce reliable estimation of mCV (Hunter et al. 1987). However, a bipolar configuration may also cause spectral dips, introducing distortion in the shape of the action potential waveforms. Yet, with a typical $CV=5$ m/s (Davies & Parker 1987) and the adopted inter-electrode distance (IED) of 32 mm for RMS estimation, the spectral dips occur at $CV/IED = 156$ Hz and its harmonics (Farina & Negro 2007b), producing negligible effect on the RMS calculation.

The results showed that mCV increased significantly after superimposing vibration on isometric contraction as compared to the control condition. mCV can be influenced by many factors, such as type and diameter of muscle fibers, pH value, and ion concentrations (Merletti & Parker 2004, Brody et al. 1991, Morimoto & Masuda 1984). Since the VE was performed at low forces, presumably with absence of fatigue (30 s duration), the changes in pH value and ion concentration were likely negligible. The increase in mCV may therefore indicate that vibration altered MU recruitment. Vibration-induced activation of larger and faster MUs may therefore be considered as the dominant mechanism contributing to the observed increase in mCV.

In our study, we did not observe significant changes in MF and therefore MF results were not correlated to the mCV values. This further indicates that MF is not an indicator of MU recruitment, as extensively discussed in previous studies and shown in experimental data (Farina et al. 2002, Martinez-Valdes et al. 2016).

The increase in sEMG amplitude with vibration indicates an increase in muscle activation. However, a significant difference between vibration conditions and baseline could only be observed at high levels of vibration, i.e., 25% and 50% of the baseline, compared to the control condition. In a previous study on the effects of a 28-Hz vibration stimulus on the biceps brachii muscle activity (Mischi & Cardinale 2009), it was suggested that the superimposed vibration is effective when added to high-level muscle tension (over 70% MVC). This can explain why RMS estimated at the lowest vibration amplitude (12.5% MVC) did not show significant differences compared to the control condition. However, limitations in the capacity of amplitude measure to infer recruitment strategies and neural activation may be an additional reason for the present results (Martinez-Valdes et al. 2018).

In summary, the observed increase in mCV can most probably be explained by vibration-induced activation of larger and faster MUs. Since MF is more sensitive to the spatial location of the activated muscle fibers as compared to muscle-fiber CV (Farina et al. 2002), no significant increase was observed in MF during VE. In addition, significant differences in RMS were only observed at the two highest vibration amplitude levels, which may reflect the dependency of the effect of VE on the initial contraction level of the muscle.

5. Conclusion

In the present study, the effects of vibration on MU recruitment patterns during low-intensity VE was investigated by analysis of sEMG features (mCV, MF, and RMS) recorded from the biceps brachii. The increase in mCV with vibration might be caused by the recruitment of larger and faster MUs. Also, the increase in EMG amplitude might suggest greater muscle activation during vibration. In conclusion, vibration superimposed on low-level isometric contraction may elicit the recruitment of larger and faster MUs and, therefore, increase the activation level of the biceps brachii muscle. To better understand these mechanisms, further studies should be carried out to analyze the activation of single MU during VE using more advanced signal processing techniques, such as sEMG decomposition (Negro et al. 2016).

References

- Abercromby A F, Amonette W E, Layne C S, Mcfarlin B K, Hinman M R and Paloski W H 2007 Variation in neuromuscular responses during acute whole-body vibration exercise. *Med Sci Sports Exerc* **39** 1642–1650
- Andreassen S and Arendt-nielsen L 1985 Fatigue of motor units in the human anterior tibial muscle. *J Appl Physiol* **61** S59

- Bongiovanni L, Hagbarth K and Stjernberg L 1990 Prolonged muscle vibration reducing motor output in maximal voluntary contractions in man. *J Physiol* **423** 15–26
- Bosco C, Cardinale M and Tsarpela O 1999 Influence of vibration on mechanical power and electromyogram activity in human arm flexor muscles. *Eur J Appl Physiol* **79** 306–311
- Bosco C, Cardinale M, Tsarpela O, Colli R, Tihanyi, J. and Von Duvillard S and Viru A 1998 The influence of whole body vibration on the mechanical behavior of skeletal muscle. *Biol. Sport.* **153** 157–164
- Brody L, Pollock M and Roy S 1991 ph induced effects on median frequency and conduction velocity of the myoelectric signal. *J Appl Physiol* **71** 1878–85
- Cardinale M and Lim J 2003 The acute effects of two different whole body vibration frequencies on vertical jump performance. *Med Sport* **56** 287–292
- Davies S W and Parker P A 1987 Estimation of myoelectric conduction velocity distribution. *IEEE Trans Biomed Eng* **34** 365–374
- Del Vecchio A, Negro F, Felici F and Farina D 2017 Associations between motor unit action potential parameters and surface emg features. *J Appl Physiol* **123** 835–843
- E Henneman G S and Carpenter D O 1965 Functional significance of cell size in spinal motoneurons. *J Neurophysiol* **28** 560–580
- Eklund G and Hagbarth K 1966 Normal variability of tonic vibration reflexes in man. *Exp Neurol* **16** 80–92
- Farina D and Merletti R 2004 Methods for estimating muscle fibre conduction velocity from surface electromyographic signals. *Med Biol Eng Comput* **42** 432–445
- Farina D and Negro F 2007a Estimation of muscle fiber conduction velocity with a spectral multidip approach. *IEEE Trans Biom Eng* **54** 1583–1589
- Farina D and Negro F 2007b Estimation of muscle fiber conduction velocity with a spectral multidip approach. *IEEE Trans Biomed Eng* **54** 1583–1589
- Farina D, Fosci M and Merletti R 2002 Motor unit recruitment strategies investigated by surface emg variables. *J Appl Physiol* **92** 235–247
- Farina D, Merletti R and Enoka R 2004 The extraction of neural strategies from the surface emg. *J Appl Physiol* **96** 1486–1495
- Farina D, Muhammad W, Fortunato E, Meste O, Merletti R and Rix H 2001 Estimation of single motor unit conduction velocity from surface electromyogram signals detected with linear electrode arrays. *Med Biol Eng Comput* **39** 225–236
- Farina D, Pozzo M, Merlo E, Bottin A and Merletti R 2004 Assessment of average muscle fiber conduction velocity from surface EMG signals during fatiguing dynamic contractions. *IEEE Trans Biomed Eng* **51** 1383–1393
- Farina D, Zagari D, Gazzoni M and Merletti. R 2004 Reproducibility of muscle-fiber conduction velocity estimates using multichannel surface emg techniques. *Muscle Nerve* **29** 282–291
- Fratini A, Cesarelli M, Bifulco P and Romano M 2009 Relevance of motion artifact in electromyography recordings during vibration treatment. *J Electromyogr Kinesiol* **19** 710–718
- Hagbarth K and Eklund G 1966 Tonic vibration reflexes (tvr) in spasticity. *Brain Res* **2** 201–203
- Hori Y, Hiraga K and Watanabe S 1989 The effects of thiamyl sodium on the tonic vibration reflex in man. *Brain Res* **497** 291–295
- Hunter I, Kearney R and Jones L 1987 Estimation of the conduction velocity of muscle action potentials using phase and impulse response function techniques. *Med Biol Eng Comput* **25** 121–126
- Krause A, Gollhofer A, Freyler K, Jablonka L and Ritzmann R 2016 Acute corticospinal and spinal modulation after whole body vibration. *J Musculoskelet Neuronal Interact* **16** 327–338
- Li W and Sakamoto K 1996 The influence of location of electrode on muscle fiber conduction velocity and emg power spectrum during voluntary isometric contraction measured with surface array electrodes. *Applied Human Science* **15** 25–32
- Lienhard K, Cabasson A, Meste O and Colson S 2015 semg during whole-body vibration contains motion artifacts and reflex activity. *J Sports Sci Med* **14** 54–61

- Lynn P 1979 Direct on-line estimation of muscle fiber conduction velocity by surface electromyography. *IEEE Trans Biomed Eng* **26** 564–571
- Martin B and Park H 1997 Analysis of the tonic vibration reflex: influence of vibration variables on motor unit synchronization and fatigue. *Eur J Appl Physiol Occup Physiol* **75** 504–511
- Martinez-Valdes E, GuzmanVenegas R A, Silvestre R A, Macdonald J H, Falla D, Araneda O F and Haichelis D 2016 Electromyographic adjustments during continuous and intermittent incremental fatiguing cycling . *Scand J Med Sci Sports* **26** 1273–1282
- Martinez-Valdes F, Negro F, Falla D, De Nunzio A and Farina D 2018 Surface electromyographic amplitude does not identify differences in neural drive to synergistic muscles. *J Appl Physiol* **124** 1071–1079
- Matthews P B C 1966 The reflex excitation of the soleus muscle of the decerebrate cat caused by vibration applied to its tendon. *J Physiol* **184** 450–472
- McGill K C and Dorfman L J 1984 High-resolution alignment of sampled waveforms. *IEEE Trans Biomed Eng* **31** 462–468
- Merletti R and Parker P 2004 *Electromyography: physiology, engineering, and noninvasive applications*. John Wiley & Sons
- Mischi M and Cardinale M 2009 The effects of a 28-hz vibration on arm muscle activity during isometric exercise. *Med Sci Sports Exerc* **41** 645–653
- Morimoto S and Masuda T 1984 Dependence of conduction velocity on spike interval during voluntary muscular contraction in human motor units. *J Appl Physiol* **53** 191–195
- Naeije M and Zorn H 1983 Estimation of action potential conduction velocity in human skeletal muscles using the surface emg cross-correlation technique. *Electromyogr Clin Neurophysiol* **23** 73–85
- Negro F, Muceli S, Castronovo A M, Holobar A and Farina D 2016 Multi-channel intramuscular and surface emg decomposition by convolutive blind source separation. *J Neural Eng* **13** 026027
- Parker P and Scott R 1973 Statistics of the myoelectric signal from monopolar and bipolar electrodes. *Med Biol Eng* **11** 591–596
- Poston B, Holcomb W and Guadagnoli M 2007 The acute effects of mechanical vibration on power output in the bench press. *J Strength Cond Res* **21** 199–203
- Rabotti C, Mischi M, Oei S G and Bergmans J W M 2010 Noninvasive estimation of the electrohysterographic action-potential conduction velocity. *IEEE Trans Biomed Eng* **57** 2178–2187
- Ribot-Ciscar E, Rossi-Durand C and Roll J 2000 Increase muscle spindle sensitivity to movement during reinforcement manoeuvres in relaxed human subjects. *J Physiol* **523** 271–282
- Ritzmann R, Kramer A, Gruber M, Gollhofer A and Taube W 2010 Emg activity during whole body vibration: motion artifacts or stretch reflexes? *Eur J Appl Physiol* **110** 143–151
- Roelants M, Verschueren S M, Delecluse C, Levin O and Stijnen V 2006 Whole-body-vibration-induced increase in leg muscle activity during different squat exercises. *J Strength Cond Res* **20** 124–129
- Romaiguère P, Vedel J P, Azulay J P and Pagni S 1991 Differential activation of motor units in the wrist extensor muscles during the tonic vibration reflex in man. *J Physiol (Lond)* **444** 645–667
- Romano M, Fratini A, Gargiulo G D, Cesarelli M, Iuppariello L and Bifulco P 2018 On the power spectrum of motor unit action potential trains synchronized with mechanical vibration. *IEEE Trans Neural Syst Rehabil Eng* **26** 646–653
- Sammali F, Xu L, Rabotti C, Cardinale M, Xu Y, van Dijk J, Zwartz M, Prete Z D and Mischi M 2018 Effects of vibration-induced fatigue on the h-reflex. *J Electromyography Kinesiol* **39** 134 – 141
- Semmler J 2002 Motor unit synchronization and neuromuscular performance. *Exerc Sport Sci Rev* **30** 8–14
- Sörnmo L and Laguna P 2005 *Biomedical signal processing in cardiac and neurological applications*. Elsevier Academic Press
- Xu L, Cardinale M, Rabotti C, Beju B and Mischi M 2016 Eight-week vibration training of the elbow flexors by force modulation: Effects on dynamic and isometric strength. *J Strength Cond Res* **30** 739–746

- Xu L, Rabotti C and Mischi M 2013 Novel vibration-exercise instrument with dedicated adaptive filtering for electromyographic investigation of neuromuscular activation. *IEEE Trans Neural Syst Rehabil Eng* **21** 275–282
- Xu L, Rabotti C and Mischi M 2015 On the nature of the electromyographic signals recorded during vibration exercise. *Eur J Appl Physiol* **115** 1095–1106
- Xu L, Rabotti C and Mischi M 2016 Analysis of vibration exercise at varying frequencies by different fatigue estimators. *IEEE Trans Neural Syst Rehabil Eng* **24** 1284–1293
- Xu L, Rabotti C and Mischi M 2017 Towards real-time estimation of muscle-fiber conduction velocity using delay-locked loop. *IEEE Trans Neural Syst Rehabil Eng* **25** 1453–1460